

The calculation of adhesive fracture energies from double-cantilever beam test specimens

B. BLACKMAN, J. P. DEAR, A. J. KINLOCH, S. OSIYEMI

Department of Mechanical Engineering, Imperial College of Science, Technology and Medicine, Exhibition Road, London SW7 2BX, UK

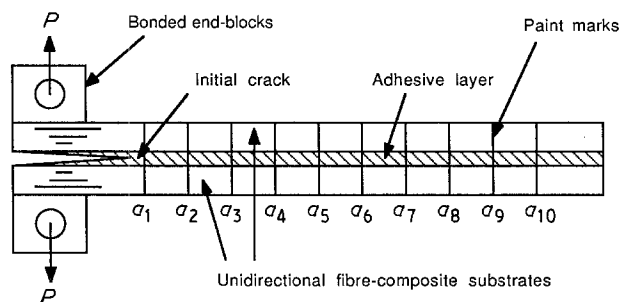
The concepts of continuum fracture mechanics have been widely employed in studies concerned with crack growth in adhesive joints [1]. Of the various test specimens that have been used to measure the adhesive fracture energy, G_a , the double-cantilever beam (DCB) specimen, which is shown schematically in Fig. 1, has been one of the most popular. The purpose of this letter is to demonstrate that, when using the DCB test specimen to study joints that consist of bonded polymeric fibre-composite substrates, careful attention needs to be paid to the method used to analyse the experimental data.

Assuming that the specimen behaves in a linear-elastic manner upon loading, there are four different linear-elastic fracture-mechanics (LEFM) methods for analysing the data contained in the load-displacement traces.

First, the "area" method, where for elastic behaviour the value of G_a may be defined by

$$G_a = \frac{\Delta U}{B\Delta a} \quad (1)$$

where B is the width of the DCB specimen and, for example, ΔU_1 is the area under the load-displacement trace and Δa is the increase in crack length from a_1 to a_2 , as shown in Fig. 2. Now when the loading and unloading relations are linear, the



Arrangement of the end-block

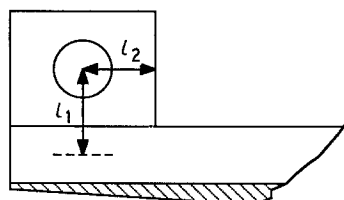


Figure 1 The double cantilever beam (DCB) adhesive joint specimen

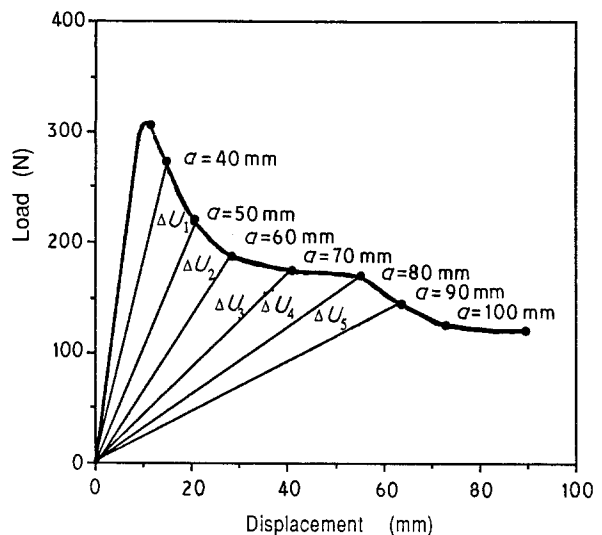


Figure 2 Typical load P , versus displacement, δ , trace for the DCB specimen using a two-part cold-cure epoxy-paste adhesive bonding poly(etherether ketone) unidirectional carbon-fibre composites.

LEFM approach may be used and, for example

$$\Delta U_1 = U_2 - U_1 = 0.5(P_1\delta_2 - P_2\delta_1) \quad (2)$$

where P_1 and δ_1 are the load and displacement, respectively, at a crack length a_1 , and P_2 and δ_2 are the respective values at a crack length a_2 .

Secondly, the "compliance" method, where from Irwin and Kies [2] the value of the adhesive fracture energy, G_a , from an LEFM test is given by

$$G_a = \frac{P^2}{2B} \frac{dC}{da} \quad (3)$$

where P is the load and C is the compliance, given by

$$C = \delta/P \quad (4)$$

where δ is the displacement corresponding to a load P . To evaluate G_a via the "compliance" method, a plot of C versus the crack length, a , may be constructed. The plot of C against a is then curve-fitted using an appropriate polynomial function, and differentiated. Then, knowing the values of the load, P , and the differential, dC/da , at a given crack length, the value of G_a as a function of the crack length may be evaluated using Equation 3.

From simple beam theory, a third approach to analysing the data is possible, since the value of the compliance, C , is given by

$$C = \frac{\delta}{P} = \frac{2a^3}{3E_s I} \quad (5a)$$

Now, when $E_s \gg E_a$, then $I \approx Bh^3/12$ and

$$C = \frac{8a^3}{BE_s h^3} \quad (5b)$$

where E_s is the flexural modulus of the fibre-composite substrate arms, which are now assumed to act as simple beams, and E_a is the modulus of the adhesive layer, I is the second moment of area and h is the thickness of a fibre-composite arm of the DCB specimen. Hence, from Equations 3 and 5a

$$G_a = \frac{P^2 a^2}{BE_s I} \quad (6a)$$

which may also be expressed as

$$G_a = \frac{12P^2 a^2}{B^2 h^3 E_s} \quad (6b)$$

Fourthly, the ‘‘displacement’’ method, where substitution for P from Equation 5a into Equation 6a yields

$$G_a = \frac{3P\delta}{2Ba} \quad (7)$$

Now as long as the load-displacement relationships for the specimen are linear for loading and unloading at any given crack length, which is true for all of the present work, then any of the four methods described above should give identical results. Furthermore, another cross-check on the analysis methods is provided by calculating the value of the modulus, E_s , of the substrate arms. This is given by

$$E_s = \frac{8Pa^3}{Bh^3 \delta} \quad (8)$$

and may obviously be compared with the value obtained by direct experimental measurements of a beam of the substrate.

Now, compared with metallic substrates, the use of polymeric fibre-composite substrates may give rise to several sources of error upon analysing the data employing Equations 6, 7 and 8. First, the relatively low shear modulus of the fibre-composite substrate arms leads to rotations and deflections occurring at the crack tip. Such effects are ignored in the simple beam analyses, which assume that the compliance at the crack root is zero, i.e. the arms act as built-in cantilever beams. Secondly, substrate arms prepared from fibre-composites tend to be slender beams and often undergo large, albeit linear, displacements during the fracture test. Also, the end-blocks which are bonded to the composite substrate arms, through which the loads are applied (see Fig. 1) tilt as the arm is bent. Both of these effects lead to an effective shortening of the composite beam. Thirdly, a correction is also required for the stiffening effects due to the presence of the metal end-blocks.

From the work of Hashemi *et al.* [3] on the interlaminar fracture of composites using the DCB specimen, the corrections for the above effects may

be expressed for the ‘‘corrected load’’ method as

$$G_a = \frac{12FP^2(a + \chi h)^2}{B^2 h^3 E_s} \quad (9)$$

and for the ‘‘corrected displacement’’ method as

$$G_a = \frac{F}{N} \frac{3P\delta}{2B(a + \chi h)} \quad (10)$$

where F , N and χ are the various correction factors which are discussed below.

First, the correction factor χ allows for all necessary shear corrections in the DCB specimen and may be ascertained experimentally from the relationship between the measured compliance, C , of the specimen and the crack length, a . The relationship between these parameters is given by

$$C = N \frac{8(a + \chi h)^3}{Bh^3 E_s} \quad (11)$$

Hence

$$\left(\frac{C}{N}\right)^{1/3} = \left(\frac{8}{Bh^3 E_s}\right)^{1/3} (a + \chi h) \quad (12)$$

Thus, from Equation 12 the measured compliance, $(C/N)^{1/3}$, may be plotted against the corresponding value of crack length, a , and the intercept yields the value of the correction factor χ . Also, from the gradient of the line, the value of the modulus, E_s , may be obtained. Note that the modulus may also be ascertained from

$$E_s = \frac{P}{\delta} \frac{8N(a + \chi h)^3}{Bh^3} \quad (13)$$

Secondly, large displacements in the specimen cause the arm effectively to shorten. In addition, the bonded end-blocks give rise to further changes if the load-point is above the beam, since the block tilts as the arm is distorted. This shortening of the crack length may be expressed in the form of a multiplying factor that may be applied to the measured crack length, a . Thus

$$F = 1 - \theta_1(\delta/L)^2 - \theta_2(\delta l_1/L^2) \quad (14)$$

where L is the length of the specimen arms, the values of θ_1 and θ_2 are 0.3 and 1.5, respectively, and l_1 is defined as the distance of the load point above the beam axis, as shown in Fig. 1.

Thirdly, since the test specimens are loaded via end-blocks bonded to the specimen arms, a correction factor is also required to account for the stiffening effect caused by the metal end-blocks. This correction factor is most conveniently expressed in the form of a correction factor N by which the displacement, δ , may be divided. In this form the correction factor N also includes (in the last two terms) the corrections needed for the large displacement and the end-block tilting effects. Thus

$$N = 1 - \theta_3(l_2/L)^3 - \theta_4(\delta l_1/L^2) - \theta_5(\delta/L)^2 \quad (15)$$

where the values of θ_3 , θ_4 and θ_5 are 1, $9.8[1 - (l_2/a)^2]$ and $9/35$, respectively.

Details of the preparation of the double-cantilever beam joints have been previously reported by

Kinloch and Kodokian [4]. Essentially, beams of unidirectional carbon-fibre composite, employing either an epoxy-based or poly(etherether ketone) matrix, were bonded using toughened epoxy adhesives. These adhesives were a two-part cold-curing paste epoxy and a single-part hot-curing film adhesive. The surface pretreatment used for the thermosetting epoxy fibre-composite substrate was as a simple abrasion/solvent-wipe, whereas a more complex "corona" treatment was necessary for the thermoplastic poly(etherether ketone) fibre-composite substrate. In all cases the surface treatment was sufficient to prevent interfacial failure occurring.

The bonded DCB specimens were tested at a displacement rate of 2 mm min^{-1} . The load-displacement trace was linear up to the start of crack propagation, and stable crack growth was observed. The crack was monitored using a travelling microscope, and as the crack propagated and crossed the markers this event was recorded on the load-displacement trace, as shown in Fig. 2. Hence, values of the adhesive fracture energy, G_a , could be determined as a function of the crack length a .

Typical results calculated from the "area" and "compliance" methods (Equations 2 and 3, respectively) are given in Table I and, as may be seen, there is a good correlation between these two basic analyses. However, when the "load" and "displacement" methods based on the assumptions of simple beam theory are employed (i.e. Equations 6b and 7), then the agreement between these two methods is very poor and, furthermore, the agreement with the former two methods is also poor. Also, the "load" method results in a significant increase in the value of G_a with increasing crack length, a ; which suggests that a rising "R-curve" (i.e. resistance curve) is recorded for this joint. It should be recalled that all these values of G_a have been deduced from the same experimental load-displacement curve and, therefore, discrepancies from using the simple

beam approach cannot be ascribed to experimental error. The fact that the values of G_a based on simple (uncorrected) beam theory are in error is further revealed from a consideration of the values of the substrate modulus, E_s , also calculated using simple beam theory, i.e. from Equation 8. These data show that the value of E_s so deduced appears to vary with the crack length; obviously this is an incorrect conclusion.

The values of G_a deduced using the corrected beam theory analyses are also shown in Table I; values from using both the "corrected load" (Equation 9) and "corrected displacement" methods (Equation 10) are included. In these equations the values of the correction factors F and N were calculated from Equations 14 and 15, respectively, and values of these terms are given in Table I. It should be noted that for relatively long cracks these correction factors make a significant difference, particularly to the "load" method (see Equation 10). The value of the crack-tip rotation and deflection correction term, χ , was ascertained using Equation 12. The plot of $(C/N)^{1/3}$ versus the corresponding value of the crack length, a , is shown in Fig. 3. As may be seen, an excellent linear fit to the data exists with a correlation coefficient of 0.999. The intercept yields a value of $\chi = 4.03$. The values of G_a deduced using the "corrected load" (Equation 9) and "corrected displacement" methods (Equation 10) are in good agreement with one another, and are in good agreement with the values from the "area" and "compliance" methods (which are, of course, unaffected by the correction factors). Furthermore, the use of the "corrected load" method reveals that, in fact, no "R-curve" actually exists for these joints. The values of E_s calculated from the corrected beam theory method (i.e. using Equation 13) are now no longer dependent on the crack length and the average value is $128.2 \pm 2.5 \text{ GPa}$. (It should be noted that this average value may also be calculated by measuring the gradient of the slope from a plot

TABLE I Values of the adhesive fracture energy, G_a , and substrate modulus, E_s , calculated from the different methods of analysis

Crack length (mm)	Values of adhesive fracture energy, G_a (kJ m^{-2})						Values of modulus, E_s (GPa)				F	N
	Area (2)	Comp. (3)	Load (6b)	Displ. (7)	Corr. Load (9)	Corr. Displ. (10)	Uncorr. (8)	Corr. (13)	(14)	(15)		
35		5.72	4.91	6.55	5.47	5.33	90.8	128.9	0.82	0.85		
40	5.86	5.68	5.11	6.52	5.43	5.38	94.8	126.8	0.82	0.85		
45	5.08	5.45	5.12	6.10	5.31	5.11	101.6	130.5	0.82	0.86		
50	5.18	5.28	5.18	5.91	5.23	5.01	106.1	131.2	0.82	0.86		
55	5.43	5.43	5.55	6.15	5.40	5.24	109.3	129.5	0.81	0.85		
60	4.92	5.14	5.45	5.77	5.23	4.96	114.4	132.3	0.81	0.85		
65	5.24	4.93	5.42	5.62	5.08	4.87	116.6	131.2	0.80	0.84		
70	5.83	5.66	6.43	6.60	5.69	5.70	117.8	125.4	0.77	0.81		
75	5.65	6.09	7.13	7.06	6.06	6.09	122.1	125.1	0.75	0.80		
80	5.96	6.59	7.92	7.57	6.46	6.52	126.6	124.5	0.72	0.78		
90	6.15	5.77	7.29	6.66	5.87	5.78	132.8	127.6	0.73	0.78		
95	5.80	5.69	7.36	6.58	5.80	5.73	135.5	127.3	0.72	0.77		
100	5.28	5.15	6.80	5.93	5.41	5.20	138.8	130.6	0.73	0.78		
105	5.63	5.47	7.38	6.36	5.59	5.54	140.4	126.8	0.70	0.75		
110	5.60	5.43	7.46	6.33	5.53	5.51	142.75	126.0	0.69	0.74		

Notes: Substrate: "corona" treated poly(etherether ketone) with the matrix containing unidirectional carbon fibres. The thickness of composite substrate arms was 1.62 mm. Adhesive: cold-cured two-part paste epoxy. The locus of joint failure was in the adhesive layer. The number under heading indicates the equation number employed in the calculation.

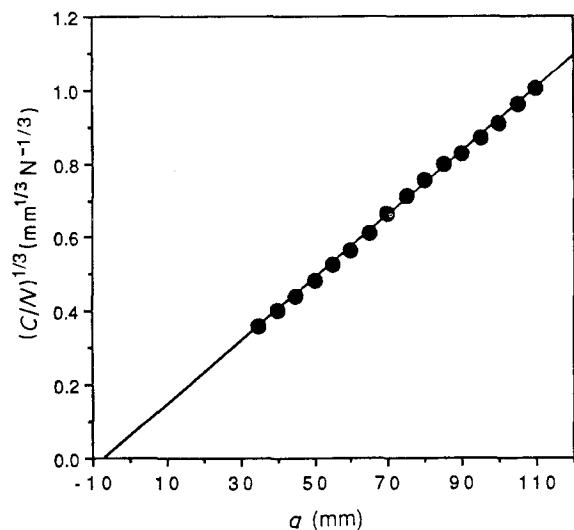


Figure 3 $(C/N)^{1/3}$ versus the crack length, a .

such as shown in Fig. 3 and using Equation 12.) This value is in excellent agreement with the independently measured value of 125 GPa for this fibre composite having the same volume fraction of fibres (i.e. 0.65%).

Finally, it should be noted that we have recorded similar observations to those reported above from a range of different fibre-composite substrate/adhesive combinations [5, 6].

In conclusion, we have shown that when deducing the results from DCB test specimens consisting of bonded polymeric fibre-composite substrates, particular attention must be given to the form of analysis that is employed for calculation of the adhesive fracture energy, G_a , and substrate modulus, E_s . However, the corrected beam theory

analyses which we have previously applied to the interlaminar failure of fibre-composites may be equally successfully employed for bonded fibre-composite joints and yield accurate and reliable values for both G_a and E_s .

Our current work is concerned with the high-rate [5] and dynamic-fatigue [6] fracture of such joints, and in these areas the adhesive fracture energy cannot be readily determined using either the "area" or "compliance" methods. Thus, the corrected beam theory methods outlined in this letter become an invaluable tool.

Acknowledgements

We thank the UK Ministry of Defence and the US Government through its European Research Office of the US Army for support and sponsorship of the present work; particularly research studentships for S.O and B.B, respectively.

References

1. A. J. KINLOCH, "Adhesion and adhesives: science and technology" (Chapman and Hall, London, 1987) p. 264.
2. G. R. IRWIN and J. A. KIES, *J. Welding* **33** (1954) 193.
3. S. HASHEMI, A. J. KINLOCH and J. G. WILLIAMS, *Proc. R. Soc. A* **427** (1990) 173.
4. A. J. KINLOCH and G. K. A. KODOKIAN, *J. Adhesion* **29** (1989) 193.
5. B. BLACKMAN, J. P. DEAR and A. J. KINLOCH, to be published.
6. A. J. KINLOCH and S. OSIYEMI, in Proceedings of Adhesion '90 (Plastics and Rubber Institute, London 1990).

Received 10 July
and accepted 1 August 1990